Cbp-dependent histone acetylation mediates axon regeneration induced by environmental enrichment after spinal cord injury in rodents

Thomas H. Hutson[1], **Claudia Kathe**[2,3], **Ilaria Palmisano**[1], **Kay Bartholdi**[3], **Arnau Hervera**[1], **Francesco De Virgiliis**[1], **Eilidh McLachlan**[1], **Luming Zhou**[1,4], **Guiping Kong**[1,4], **Quentin Barraud**[3], **Matt C. Danzi**[5], **Alejandro Medrano-Fernandez**[6], **Jose P. Lopez-Atalaya**[6], **Anne L. Boutillier**[7], **Sarmistha H. Sinha**[8], **Akash K. Singh**[8], **Piyush Chaturbedy**[9], **Lawrence D. F. Moon**[2], **Tapas K. Kundu**[8], **John L. Bixby**[5], **Vance P. Lemmon**[5], **Angel Barco**[6], **Gregoire Courtine**[3,#], **Simone Di Giovanni**[1,4,#,*]

[1.]Centre for Restorative Neuroscience, Division of Brain Sciences, Department of Medicine, Imperial College London, London, W12 0NN, UK. [2.]Neurorestoration Group, Wolfson Centre for Age-Related Diseases, King's College London, London, SE1 1UL, UK. [3.]Brain Mind Institute and Center for Neuroprosthetics, Ecole Polytechnique Fédérale de Lausanne (EPFL), 1202 Geneva, Switzerland. [4.]Hertie Institute for Clinical Brain Research, University of Tubingen, Tubingen, Germany. [5.]The Miami Project to Cure Paralysis, University of Miami, Miami, FL 33136, USA. [6.]Instituto de Neurociencias, Universidad Miguel Hernandez Consejo Superior de Investigaciones Científicas, 03550 Alicante, Spain. [7.]Université de Strasbourg, CNRS, UMR 7364, Laboratoire de Neuroscience Cognitives et Adaptatives (LNCA), F-67000 Strasbourg, France. [8.]Transcription and Disease Laboratory, Jawaharlal Nehru Centre for Advanced Scientific Research, Bangalore 560064, India. [9.]Nanomaterials and Catalysis Laboratory, Chemistry and Physics of Materials Unit, JNCASR, Bangalore 560064, India.

Abstract

[*]Correspondence: s.di-giovanni@imperial.ac.uk. Centre for Restorative Neuroscience, Division of Brain Sciences, Department of Medicine, Imperial College London, London, W12 0NN, UK.
[#]Co-senior authors

Following a spinal cord injury, axons fail to regenerate in the adult mammalian central nervous system, leading to permanent deficits in sensory and motor functions. Increasing neuronal activity after an injury using electrical stimulation or rehabilitation can enhance neuronal plasticity and result in some degree of recovery; however the underlying mechanisms remain poorly understood. We found that placing mice in an enriched environment prior to an injury enhanced the activity of proprioceptive dorsal root ganglion neurons leading to a lasting increase in their regenerative potential. This effect was dependent on Creb-binding protein (Cbp) mediated histone acetylation, which increased the expression of genes associated with the regenerative program. Intraperitoneal delivery of a small molecule activator of Cbp at clinically-relevant times promoted regeneration and sprouting of sensory and motor axons, as well as recovery of sensory and motor functions in both a mouse and rat model of spinal cord injury. Our findings showed that the increased regenerative capacity induced by enhancing neuronal activity is mediated by epigenetic reprogramming in rodent models of spinal cord injury. Understanding the mechanisms underlying activity-dependent neuronal plasticity led to the identification of potential molecular targets for improving recovery after spinal cord injury.

One Sentence Summary:

Environmental enrichment induces activity-dependent histone acetylation via an epigenetic druggable mechanism to promote recovery after spinal cord injury.

Introduction

Following spinal cord injury (SCI), motor and sensory axons fail to regenerate, leading to permanent neurological impairments (1, 2). This absence of regeneration in the central nervous system (CNS) after injury has been attributed to two main interconnected factors: the presence of growth inhibitory molecules in the CNS and the lack of an effective neuronal-intrinsic regenerative response (2–4). Although axon regeneration fails in the CNS after injury, limited regeneration and partial functional recovery do occur in the injured peripheral nervous system (PNS) (5, 6). Dorsal root ganglion (DRG) neurons are located at the interface between the PNS and CNS. Their pseudounipolar anatomy provides the unique opportunity to study regenerative mechanisms in both locations from a single cell body. A well-established model for increasing the intrinsic regenerative capacity of DRG neurons in rodents consists of inducing a conditioning injury to the axons in the peripheral sciatic nerve prior to axons in the CNS. The peripheral injury induces the expression of regeneration associated genes (RAGs) that increases the regenerative potential of the DRG neurons eliciting a stronger regenerative response after CNS injury (7–9). Although this has provided useful insights in the mechanisms underlying axon regeneration, a conditioning lesion only induces modest regeneration in the CNS (9) and is not a clinically viable approach.

Sensory DRG neurons convey afferent information from the periphery to the spinal cord in order to modulate motor outputs, and to supraspinal structures for the elaboration of sensorimotor integration and conscious perception. Amongst the DRG, proprioceptive neurons innervate muscle spindles and Golgi tendon organs (10). They transmit information about the length and tension of muscles, which plays a critical role during sensorimotor execution (11, 12). Proprioceptive afferent feedback influences the activity of circuits in the

spinal cord and plays an essential role in providing immediate adjustment and refinement of movement and motor-learning (13). Moreover, it plays an important role in directing motor recovery after SCI. Mice lacking functional proprioceptive afferents exhibit a defective rearrangement of descending pathways that prevents recovery after SCI (12). This observation suggests that proprioceptive neurons may deliver molecular cues for axonal regrowth and sprouting after injury. In support of this hypothesis, previous studies have shown that modulation of proprioceptive afferents with electrical stimulation (14, 15) and rehabilitative training (16) augmented neuroplasticity and recovery in both animal models and humans after SCI (17). However, the underlying mechanisms remain poorly understood.

Here, we used environmental enrichment (EE) as a means to physiologically increase neuronal activity in rodents. It has been previously shown that exposing mice to EE has profound effects on the structure and function of cortical and hippocampal neurons, leading to enhanced neuroplasticity, synaptogenesis, neurogenesis and ultimately improved memory and cognitive performance (18–20). The innervation of muscle spindles and Golgi tendon organs by proprioceptors suggests that they are ideally located to be modulated by environmental stimuli.

We investigated the impact of environmental enrichment (EE) on proprioceptive DRG neurons, hypothesizing that this would prime them to initiate a regenerative response to a subsequent injury, similar to a conditioning injury. Our results showed that augmenting the activity of proprioceptive DRG neurons using EE in mice induced a lasting increase in their regenerative potential due to cAMP-response element binding protein (Creb) binding protein (Cbp) mediated histone acetylation. Pharmacologically increasing Cbp acetyltransferase activity following SCI in a mouse model, induced regeneration and sprouting of sensory axons and brainstem motor pathways resulting in improvements in both sensory and motor functions. These results show that neuronal activity leads to changes in chromatin environment that boost the regenerative capacity of neurons. Elucidating the mechanisms underlying activity-dependent responses in neurons translated into the identification of a potential treatment for SCI that warrants evaluation in humans.

Results

Environmental enrichment induces a lasting increase in the regenerative potential of DRG neurons

To test whether EE can enhance the regenerative potential of DRG neurons, mice were exposed to EE or standard housing (SH) for 1, 3, 6, 10 or 35 days. After exposure to EE, the

sciatic DRGs were cultured in a growth permissive substrate for 12 hours Neurite outgrowth of DRG neurons was enhanced after exposure to EE for 10 or 35 days (Fig. 1A and B). The extent of neurite outgrowth on a growth inhibitory myelin substrate was similar to what is observed after a conditioning injury (fig. S1).

The EE-dependent increase in neurite outgrowth was abolished when incubating the neurons with the transcriptional inhibitor actinomycin-D (fig. S2), suggesting a dependence of this response on gene transcription. EE-dependent increase in neurite outgrowth was maintained

when the animals returned to SH for 5-weeks after 10 days of EE (Fig. 1C, D and E), suggesting that EE may trigger long-lasting effects. Analyses of growth responses revealed that EE enhanced axon elongation rather than branching, which may translate into axonal regeneration in vivo (fig. S3).

Given the multifactorial nature of EE, we decided to discriminate between the relative role of running, which has previously been shown to enhance peripheral nerve regeneration (21) and the remaining environmental stimuli (larger cage, increased number of mice, novel objects, and increased nesting material) on DRG outgrowth. Mice were placed either in EE, in SH, in EE with an immobilized wheel or in SH with a running wheel for 10 days. Analysis of neurite outgrowth showed that although the running wheel in SH enhanced outgrowth compared to SH alone, the full complement of EE still induced a higher degree of outgrowth (fig. S4). This result indicated that the full EE is required for maximal enhancement of DRG outgrowth.

We next tested whether EE can also enhance regeneration of axons within the peripheral and the central nervous system. Exposing the mice to EE before sciatic nerve complete transection and reanastomosis enhanced sciatic nerve regeneration (Fig. 1F and G). The same protocol also increased muscle reinnervation after a sciatic nerve crush (fig. S5).

We then assessed whether pre-exposure to EE would enhance regeneration of sensory axons in the dorsal columns after a SCI and compared this response to the regeneration observed after a conditioning injury. Three groups of adult mice were exposed to EE or SH for 10 days and then housed in SH. Subsequently, SH mice received a conditioning sciatic nerve axotomy (SNA) or sham injury. The EE groups only received the sham injury. Next, all the mice received a thoracic (T12) dorsal hemisection. Five weeks later, the retrograde tracer Cholera Toxin subunit B (CTB) was injected into the sciatic nerves to evaluate the regeneration of ascending dorsal column axons (Fig. 1H). The majority of labelled axons from SH Sham mice retracted from the injury site. In contrast, labelled axons from EE mice could be observed within the lesion epicenter. Some regenerating axons even expanded beyond the lesion site, attaining a distance up to 800 μm from the lesion border (Fig.1H and I). Some of these regenerating axons co-localized with vesicular glutamate transporter 1 (vGlut1), a marker of presynaptic glutamatergic synapses, suggesting the formation of putative synapses (fig. S6). As expected, the conditioning injury in SH mice also promoted axonal regeneration (Fig. 1H and I).

Six weeks after injury, we conducted terminal electrophysiological experiments to evaluate the functionality of these regenerating axons. The dorsal columns were stimulated below the injury at L5, and recorded both below and above the lesion, at L1 and T9, respectively (Fig. 1J). The amplitude of the compound action potentials recorded above the lesion site was larger for the animals that had been housed in EE compared to SH or SH-SNA (black traces, Fig. 1K and L), suggesting an increase in neuroplasticity across the lesion. There was no difference in the compound action potentials recorded below the lesion for any of the groups (blue traces, Fig.1K).

To determine whether regenerating sensory axons were responsible for the increase in conduction through the lesion site, we selectively silenced these axons using designer receptors exclusively activated by designer drugs (DREADD), as described previously (22). We injected the adeno-associated viral vector (AAV) AAV-flex-hM4Di into the sciatic nerve, which will silence the activity of DRG neurons after Cre recombination. Three weeks after SCI, an AAV-Cre was injected rostral to the site at of injury to induce the expression of the Cre-dependent Gi-coupled DREADD receptor only in those DRG neurons that had extended axons through and beyond the lesion. After three additional weeks, mice previously exposed to EE underwent electrophysiological assessment. Chemogenetic mediated silencing restricted to regenerated axons (Cre-dependent AAV-flex-hM4Di) reduced conduction across the lesion, establishing causality that was confirmed with a re-transection (Fig. 1K and L).

Proprioceptive afferent feedback is required for EE-mediated increase in DRG regenerative growth

We next investigated whether a specific type of DRG neuron was implicated in EE-dependent regenerative growth. We injected CTB into the distal sciatic nerve one day after performing a sciatic nerve crush injury. Consequently, only DRG neurons that regenerated an axon across the injury site and into the denervated nerve would be able to take up the CTB tracer (Fig. 2A). Two days after the CTB injection, we assessed the number of CTB-positive DRG neurons that co-stained for markers of the main DRG subpopulations (Fig. 2B). Prior exposure to EE increased the number of CTB positive DRG neurons, confirming that EE enhances axon regeneration (Fig. 2C). The majority of DRG neurons, which regenerated axons through the sciatic nerve crush and were retrogradely labeled with CTB, expressed markers of proprioceptors (parvalbumin) rather than nociceptors (isolectin B4 or substance P) (Fig. 2B and D), suggesting that EE preferentially enhanced the regeneration of proprioceptive DRG neurons in this model.

To evaluate whether the EE-dependent increase in regenerative potential of proprioceptive neurons relied on a muscle spindle proprioceptive mechanism, we used $Egr3^{-/-}$ mice. This mutation abolishes muscle spindle proprioceptive feedback while retaining a similar number of parvalbumin (PV) DRG neurons compared to wild-type (WT) mice (12, 23) (Fig. 2E). We found that EE- but not conditioning injury-dependent DRG outgrowth was abolished in mice lacking intact muscle spindles ($Egr3^{-/-}$) (Fig. 2F and G). This observation indicates that EE-dependent regenerative priming is likely to be contingent on intact proprioceptive afferent feedback.

Finally, to further confirm the cell type specificity of the EE mechanism, we assessed neurite outgrowth of DRG neurons from mice that expressed the fluorescent marker tdTomato under the control of the PV promoter. Exposure to EE significantly increased the outgrowth of tdTomato positive (PV^{ON}) but not tdTomato negative (PV^{OFF}) DRG neurons (Fig. 2H and I).

Taken together, these experiments demonstrate that prior exposure to EE primes proprioceptive DRG neurons for enhanced axon regeneration.

Environmental enrichment induced signaling pathways involved in neuronal activity, calcium mobilization and the regenerative program of large-diameter DRG neurons

EE and exercise have been shown to increase neurotrophin expression and modify cytokines influencing neuroplasticity (21, 24–26). Surprisingly we found no changes in neurotrophin or cytokines levels in the DRG or in the blood (fig. S7), suggesting that alternative mechanisms may be responsible for EE-dependent DRG regenerative growth.

To uncover EE-dependent molecular mechanisms, we performed RNA sequencing (RNAseq) from whole DRG or laser-captured large-diameter DRG neurons (LDN), which represent the proprioceptor and mechanoreceptor population, as well as conducting proteomic analysis from sciatic nerve axoplasm after 10 days in EE or SH. Unsupervised gene expression clustering showed dramatic changes in gene expression of LDN after EE compared to SH, but not in the whole DRG, which contains a multitude of different neuronal and glial cell types (Fig. 3A, fig. S8A, Datafile S1). The data shows that EE preferentially increased rather than repressed gene expression in LDN (fig. S8B). Altogether, these results confirmed that EE specifically modulates gene expression in proprioceptors/mechanoreceptors. Similarly, proteomic analysis showed a larger number of up-regulated proteins after EE vs SH (71 vs 49, fig. S8C and Datafile S1). Overall, 37 out of 71 up-regulated proteins were also up-regulated at the RNA level, suggesting that gene transcription drove more than half of the observed protein changes (Datafile S1). Functional classification of EE-dependent gene expression changes in LDNs revealed that EE strongly modulated functionally interconnected molecular pathways involving ion channels, neuronal activity, calcium signaling, energy metabolism and neuronal projection (Fig. 3B, fig. S8D, Datafile S2). Combined analysis of the RNAseq and proteomic datasets for protein-protein interactions identified multiple interactions between proteins involved in neuronal activity, calcium signaling and cytoskeletal rearrangements, supporting a role for EE-mediated activity in axon projection and elongation (fig. S8E).

These results encouraged us to investigate the role of neuronal activity and calcium release in the EE-mediated increase in DRG regenerative potential. We employed an AAV-mediated chemogenetics approach to inhibit or enhance neuronal activity of DRG neurons using DREADD technology. When activated by the pharmacologically inert ligand clozapine-N-oxide (CNO), Gi-coupled (hM4Di) DREADD receptors inhibit adenylyl cyclase, which silences neuronal activity (27). Alternatively, activation of Gq-coupled (hM3Dq) DREADD receptors enhance neuronal activity by eliciting IP_3-mediated calcium release from intracellular stores (27). This increase in intracellular calcium activates calcium-dependent signaling cascades, which would, if our hypothesis is correct, mimic the effects of EE on DRG neurons identified with gene and proteomic analysis.

We injected AAV vectors into the sciatic nerve to express hM4Di, hM3Dq or GFP in DRG neurons. mCitrine/GFP expression confirmed an efficient transduction (fig. S9). Four weeks after injection, mice expressing hM4Di, hM3Dq or GFP were placed in EE or SH. CNO was added in the drinking water to activate the receptors. Ten days later, we performed a sciatic nerve crush, and assessed the extent of regeneration three days post-injury (Fig. 3C and D).

Gq activation enhanced axon regeneration in SH mice and Gi-dependent inactivation of DRG neurons attenuated axon regeneration of mice exposed to EE, demonstrating the importance of neuronal activity for EE-mediated regeneration (Fig. 3C and D). Expression of Gi in SH mice or Gq in EE mice did not further impair or promote axon regeneration (Fig. 3C and D). Similar results were obtained when assessing neurite outgrowth of DRGs cultured for 12 hours after in vivo DREADD transduction and EE exposure (fig. S10). Gq expression in DRGs from SH mice increased neurite outgrowth to a similar extent to what was observed in the DRGs of mice exposed to EE, while the expression of Gi in DRG neurons reduced EE-dependent outgrowth (fig. S10).

RNAseq and proteomics data suggested that EE may enhance calcium signaling in proprioceptive DRG neurons. To visualize the induction of activity-dependent signaling pathways in proprioceptive neurons in response to EE, we directly measured intracellular calcium, as an indicator of release from intracellular stores. Transgenic mice expressing the calcium indicator genetically encoded calmodulin protein (GCaMP) under the PV promoter were exposed to EE or SH for 10 days. Whole sciatic DRGs were extracted to measure the fluorescent signals of proprioceptive neurons ex vivo when applying increasing levels of potassium chloride. As anticipated, we found that exposing the mice to EE increased the amount of calcium in DRG neurons at all the potassium chloride concentrations tested compared to DRGs from SH mice (Fig. 3E and F, Videos S1 and S2). These observations show that EE increases calcium signaling in proprioceptive neurons, likely through increased solicitation of muscle spindles and force sensors within the enriched environment.

These results provide evidence that EE increases neuronal activity and calcium signaling in proprioceptive DRG neurons and plays an important role in the activity-dependent increase in regenerative potential.

Cbp mediated histone acetylation is required for EE-dependent increase in regeneration potential

We reasoned that EE-dependent modulation of neuronal activity might induce epigenetic modifications enabling active transcription and a lasting increase in regenerative potential. Immunostaining and immunoblotting for markers of histone acetylation and methylation, which are important to regulate gene expression, showed that EE enhanced H3K27ac and H4K8ac but not H3K9ac, H3K4me2 or H3K4me3 in parvalbumin-positive DRG neurons (Fig. 4A, B and E, fig. S11). H4K8ac and H3K27ac are both well-established markers of transcriptional activation, which correlated with our RNAseq data where we observed activation of gene expression in the large-diameter sensory neurons after EE. These two histones can be acetylated by Cbp (28, 29), a lysine acetyltransferase that contains two calcium-sensitive transactivation domains (30) and is involved in activity-dependent neuroplasticity (19, 31, 32). Acetylation of Cbp increases its acetyltransferase activity and facilitates transcription complex formation and the acetylation of H4K8 and H3K27, leading to persistent changes in transcriptional activity (33, 34). EE increased pCreb (Fig. 4C, D and F) and active acetylated-Cbp (acCbp) expression in PV-positive DRG neurons (Fig. 4G and H). Levels of H4K8ac but not pCreb or acCbp remained elevated in PV[ON] DRG neurons 5 weeks after exposure to EE (fig. S12). Furthermore, the levels of H4K8ac and acCbp in

DRG neurons were enhanced or inhibited by hM3Dq or hM4Di, respectively, linking calcium-dependent neuronal activity to histone acetylation (fig. S13).

To further elucidate the role of Cbp in the EE-mediated increase in the regenerative potential of DRG neurons, we used CaMKIIa-creERT2/Cbp$^{f/f}$ transgenic mice with tamoxifen inducible Cbp deletion in CaMKIIa positive cells (19). In the DRG, CaMKIIa positive cells include large, medium and small diameter neurons (35) (fig. S14). Four weeks after tamoxifen treatment, mice were placed in EE or SH for five weeks prior to the extraction of the sciatic DRG neurons. Neurite outgrowth was then assessed after 12 hours in culture. The conditional deletion of Cbp in CaMKIIa-positive cells (19) abolished the EE-dependent increase in neurite outgrowth (Fig. 4I and J). This data suggest that Cbp specifically contributes to mediating the increase in regenerative potential of DRG neurons after EE exposure. In addition, we also found that Cbp deletion completely abolished the EE-mediated increase in H4K8ac (Fig. 4K), ruling out a substantial role for other histone acetyltransferases.

Pharmacological activation of Cbp/p300 promotes sensory axon regeneration and recovery after a dorsal hemisection SCI in mice

The central role of Cbp suggested that the pharmacological activation of Cbp might mimic the EE-dependent increase in regenerative growth of DRG neurons. To test this hypothesis, we delivered a small-molecule activator (TTK21) of the closely related transcriptional co-activators Cbp and p300 after SCI (36). Recent studies have shown that TTK21 is non-toxic in animal models, and when conjugated to glucose derived carbon nanospheres (CSP), successfully crosses the blood brain barrier, effectively enhances histone acetylation in the hippocampus, and promotes improvements in learning and memory capacities (36, 37).

We first confirmed that the addition of CSP-TTK21 to DRG cultures was capable of increasing neurite outgrowth compared to control CSP. CSP-TTK21 increased neurite outgrowth, H4K8 acetylation, and reduced neurite branching in cultured DRG neurons (Fig. 5A and B). We next tested whether CSP-TTK21 could promote axonal regeneration in vivo following a mid-thoracic dorsal hemisection (Fig. 5C). Injured mice received a weekly intraperitoneal (i.p.). injection of 20 mg/kg CSP-TTK21 or control CSP, beginning 4 hours after injury. To assess regeneration of sensory axons in the dorsal columns, we injected the sciatic nerves with CTB tracer and examined the spinal cord six weeks after SCI (Fig. 5D). Treatment with CSP-TTK21 promoted sensory axon regeneration up to 1000 μm rostral to the lesion (Fig. 5E and F). We conducted behavioral assessments for five weeks after SCI to evaluate recovery of sensorimotor function. We selected tasks contingent on accurate proprioceptive information, which included the Gridwalk and adhesive tape test. We observed a decrease in the number of hindlimb slips in the gridwalk test (Fig. 5G) and a superior recovery in the time it took to sense and then remove a piece of adhesive tape placed on the hindpaws after treatment with CSP-TTK21 (Fig. 5H, fig. S15). Many of the regenerating axons from the CSP-TTK21 treated mice co-localized with vGlut1, suggesting the formation of putative synapses (Figure 5I, J and K). We then assessed the functionality of these regenerating axons with terminal electrophysiological experiments. We found an increase in the amplitude of compound action potentials recorded above the SCI in treated

mice compared to the control group, demonstrating that the Cbp activator increased neural conduction across the lesion site (Fig. 5L and M). In addition to promoting axon regeneration across the lesion site, we investigated whether CSP-TTK21 also increased sprouting of axons below the level of injury. CSP-TTK21 enhanced the number of vGlut1-positive boutons apposed to motoneurons (putative synapses) in the ventral horn of the lumber enlargement (Fig. 5N and O), suggesting spinal circuit reorganization and sprouting of group-Ia proprioceptive afferents below the injury. This reorganization of proprioceptive afferents has previously been associated with functional recovery (12, 16). We also observed an increase in the intensity of vGlut1 staining in lamina V of the spinal cord after CSP-TTK21 treatment (fig. S16). In addition, CSP-TTK21 treatment increased H4K8 acetylation within DRG neurons (fig. S17), but did not affect the area or intensity of glial fibrillary acidic protein (Gfap) staining, a marker of the inhibitory astrocytic scar that surrounds the lesion site (fig. S18).

Pharmacological Cbp/p300 activation enhances sprouting of both descending motor and ascending sensory axons leading to functional recovery after contusion SCI in rats

To further substantiate the efficacy of CSP-TTK21 in vivo, we evaluated whether CSP-TTK21 could promote anatomical and functional neuroplasticity of motor systems after a more clinically relevant SCI. Adult rats underwent a mid-thoracic spinal cord contusion (220 kdyn). CSP-TTK21 or CSP was administered i.p. 6 hours after SCI, and repeated weekly thereafter.

To quantify locomotor performance, we applied a principal component (PC) analysis to various parameters (fig. S19) calculated from kinematic recordings of quadrupedal walking along a flat corridor. PC1 captured the extent of the recovery, showing that CSP-TTK21 significantly (P=0.0002) improved locomotor performance compared to CSP-treated rats. Parameters that correlated with improved recovery included reduced paw dragging, increased step height and more frequent plantar steps with weight bearing (Fig. 6A–D, Video S3). The number of footfalls occurring during locomotion across a horizontal ladder also decreased (fig. S20). This functional recovery was associated with increased sprouting of descending reticulospinal and serotoninergic axons within the lumbar spinal cord (Fig. 6E–J). Consistent with this, CSP-TTK21 enhanced H4K8ac in the reticular formation and raphe nucleus (fig. S21). CSP-TTK21 also augmented the density of vGlut1-positive boutons from proprioceptors onto motoneurons located within lumbar segments below the injury (Fig. 6K and L), which was associated with increased muscle responses evoked by stimulating proprioceptive afferents (H-reflex, Fig. 6M). However, CSP-TTK21 did not affect the lesion size or Gfap intensity (fig. S22).

Together, these results show that activating Cbp using a small-molecule promotes sprouting of descending pathways and proprioceptive afferents below injury and improved recovery of both sensory and motor functions after a contusion SCI in rats.

Discussion

Our work suggests that increasing the neuronal activity of proprioceptive DRG neurons prior to an injury using EE or chemogenetics elicits Cbp-mediated histone acetylation that is

required for an enduring increase in axonal regeneration potential. Activating Cbp using a small-molecule at clinically relevant time points in both mouse and rat models of SCI mimicked the effect of increasing neuronal activity. CSP-TTK21 treatment promoted regeneration of ascending sensory axons and sprouting of both sensory and supraspinal motor axons below the lesion. The induced spinal circuit reorganization resulted in electrophysiological and behavioral recovery. The complete lack of EE-mediated increase in neurite outgrowth observed in DRGs from $Egr3^{-/-}$ mice with defective muscle spindle receptors demonstrates the importance of proprioceptive neurons and muscle spindle afferent feedback in triggering the activity-dependent increase in regeneration potential. This finding provides evidence and expands upon the recent demonstration that muscle spindle feedback is essential for inducing the correct anatomical reorganization of projection neurons and functional recovery after spinal cord injury (12). In addition to the $Egr3^{-/-}$ mice we used CTB tracing and PV-tdTomato mice to provide further evidence to support this remarkable cell type specificity. Furthermore, we found that EE drives the expression of genes underlying neuronal activity, calcium signaling and regenerative pathways in large-diameter DRG neurons. Indeed, the robust gene expression response was largely lost when RNAseq was performed from the whole DRG that contains multiple neuronal populations and glial cells. This highlights the specificity of EE-mediated gene-expression in large-diameter DRG neurons, which mainly constitute proprioceptors and mechanoreceptors. The impact of neuronal activity on axon regeneration could be reproduced experimentally. We showed that the manipulation of DRG neuronal activity using chemogenetics reproduced or abolished the EE-mediated increase in axonal regeneration potential. Furthermore, the increase in DRG neuronal activity alone triggered an increase in axon regeneration, further expanding upon what has been observed recently (38, 39). Together, these data suggest that the effects of EE are essentially elicited by proprioceptive feedback signals, which leads to an enhanced activity of proprioceptive DRG neurons that promotes a lasting augmentation of their regenerative potential.Next, our results provided evidence that the lasting increase in regeneration potential is mediated by a Cbp-dependent increase in histone acetylation and a marked increase in gene expression, including pathways involved in neuronal activity, axonal projection and cytoskeleton remodeling. Specifically, neuronal activity elicited by EE activates Cbp and increases the acetylation of H4K8. This enduring increase in histone acetylation likely mediates the long-lasting enhancement in regenerative potential of these DRG neurons that extends for several weeks. The levels of histone acetylation are likely maintained because they do not rely solely upon the histone deacetylase/acetyltransferase equilibrium but on the overall epigenetic configuration of the locus. While this is important for histones, it is unlikely for proteins, such as Cbp, whose acetylation status directly depends on the activity of signal transduction pathways. The requirement of Cbp was confirmed by deletion, which completely abrogated the EE-mediated increase in DRG neurite outgrowth and H4K8 acetylation. Furthermore, pharmacological activation of Cbp after SCI promoted axonal regeneration and functional recovery. These data suggest that Cbp is necessary for the EE-mediated increase in DRG neurite outgrowth and that its activation promotes functionally relevant axon regeneration and sprouting leading to recovery.

Our findings expand upon recent studies by us and others showing that histone acetylation is associated with a transcriptional-dependent enhancement of the regeneration program in neurons (40–45). We previously demonstrated that a conditioning injury activates p300/Cbp associated factor (Pcaf). Together with HAT p300, Pcaf promotes acetylation of the promoters of known regeneration associated genes (RAGs), which facilitate their expression and thereby enhance axon regeneration after injury (40, 42, 43). The inhibition histone deacetylases (HDACs) promotes histone acetylation and axonal regeneration (41, 44). Similarly, nuclear export of HDAC5 has been shown to be required for peripheral axon regeneration and for the induction of a number of RAGs (45). Our present results show that EE-dependent histone acetylation does not involve Pcaf since H3K9 acetylation is not altered by EE and does not require p300, since Cbp deletion completely blocked EE-dependent DRG regenerative growth. These observations suggest that a conditioning injury and EE operate via separate signaling mechanisms leading to distinct histone acetylation changes. However, a limitation of the present and previous studies is the lack of systematic screening for post-translational histone modifications that affect the histone code and gene transcription. The systematic measurement of histone acetylation and methylation could lead to the identification of additional histone modifying enzymes that modulate EE-dependent or conditioning-dependent axonal regeneration in addition to Cbp/p300 and Pcaf. Collectively, these studies demonstrate the importance of the chromatin environment for the regenerative capacity of DRG neurons. Identifying and manipulating key histone modifiers that can orchestrate broad changes in gene transcription may lead to significant improvements in axon regeneration. The identification of the mechanisms underlying the activity-dependent increase in DRG regenerative growth allowed us to reproduce these effects pharmacologically. We show that the activation of Cbp within a clinically relevant time frame after SCI (within 6 hours) using a non-toxic small molecule promotes regeneration of ascending and descending axons. Cbp activation also triggered a robust sprouting of proprioceptive fibers below the injury, within the lumbar motor circuitry. These changes were associated with enhanced electrophysiological and behavioral functional recovery in sensory and motor tests. Although the specific contribution from each reorganized system remains unclear, we surmise that the reorganization of proprioceptive afferent feedback circuits below the injury is more important to improve precision walking than the relatively short-distance regeneration of ascending fibers. Although the specific mechanisms of recovery require to be studied further, these combined findings show that activity-dependent regenerative pathways triggered preceding a SCI can also be successfully targeted to enhance axon sprouting, regeneration and sensorimotor recovery after injury.

Rehabilitation strategies including exercises that increase afferent activity in the spinal cord are now well established to augment functional recovery in rodents after SCI, although their effect on axon regeneration in the CNS is not clear (46–48). Moreover, modulation of proprioceptive afferent circuits with electrical stimulation augments neuroplasticity and recovery after a SCI (15, 16, 49, 50). Thus, our results re-emphasized the critical role of proprioceptive neurons in steering the re-organization of neural pathways that supports functional recovery after SCI.

However, few studies have systematically investigated the impact of task-specific rehabilitation strategies prior to SCI on neuroplasticity and functional recovery. One study

demonstrated that voluntary exercise prior to peripheral nerve injury enhances peripheral nerve regeneration (21). This observation is consistent with the robust axon regeneration resulting from an exposure to EE prior to a peripheral nerve injury. The study by Molteni et al reported an increase in neurotrophin mRNA in the DRG after exercise (21). Consequently, they used a pharmacological inhibitor of Trk tyrosine kinase to demonstrate that the exercise-mediated increase in DRG outgrowth was contingent on neurotrophin release. These findings differ from our data, since we did not observe any significant increase in neurotrophin mRNA or protein levels in DRGs after exposure to an EE. Along the same lines, a recent study has shown that exercise after SCI does not change neurotrophin expression in large-diameter DRG neurons (51). It is possible that the pharmacological inhibitor of Trk tyrosine kinase may have off-target effects altering multiple intracellular signaling pathways that lead to the reduction in DRG outgrowth. Voluntary exercise has been demonstrated to prevent the reduction of key signaling molecules that are involved in neuroplasticity including pSynapsin I, pCreb and pCaMK in the spinal cord and brain (52). Similarly, we found that EE triggers an increase in calcium related signaling molecules known to be important in gene regulation and inducing neuroplasticity, such as Calbindin2 (53). Involuntary exercise was recently shown to promote axon regeneration of propriospinal neurons but not sensory DRGs after a complete transection of the spinal cord and peripheral nerve graft (PNG) (54). This suggests that unlike the Cbp activator used in the present study, increasing the activity of DRG neurons after a SCI using an exercise paradigm may be insufficient to increase the intrinsic regenerative state of the DRGs and promote sensory axon regeneration. Additionally, although we did not combine the Cbp activator with neurorehabilitation paradigms, this is worth investigating in the future since they might synergize for improved axonal plasticity and functional recovery. Although we show efficacy of the small molecule activator of Cbp in two different species and two clinically relevant models of SCI, a limitation is that rodent models of SCI cannot fully replicate the human pathology. Additionally, although we did not observe any obvious side-effects following treatment with the Cbp activator, these were not systematically assessed. Therefore future studies will be required to fully evaluate the toxicity profile of the compound before translation to clinical SCI.

Finally, it is worth speculating upon the anecdotal evidence that individuals who had an "active lifestyle" recover to a greater degree after SCI than individuals who lived "less active" lifestyles. In addition to the global benefits associated with a healthy lifestyle, our combined observations prompt us to suggest that neurons are "primed" for axonal regeneration and sprouting, which contribute to this enhanced recovery. It will be useful to collect epidemiological data supporting or refuting this hypothesis.

In summary, we have demonstrated an epigenetic-based mechanism underlying activity-dependent neuronal plasticity. The exploitation of this mechanism allowed us to utilize a pharmacotherapy that enhanced spinal cord repair and functional recovery after SCI, opening a realistic pathway for clinical evaluations.

Materials and methods

Study design

We investigated the impact of environmental enrichment (EE) on proprioceptive DRG neurons, hypothesizing that EE would prime these neurons to initiate a regenerative response to a subsequent injury. All surgical and experimental procedures on rodents were carried out in accordance with the UK Animals (Scientific Procedures) Act 1986 and approved by the veterinarian and ethical committee of Imperial College and the canton of Vaud and Geneva. Animals were assigned randomly to experimental groups and surgeries were carried out in a random block design. All analysis was performed by the same experimenter who was blinded to the experimental groups. All behavioral testing and analysis was performed by an observer blinded to the experimental groups. N values represent the number of animals in the experiment and each experiment contained a minimum of 3 technical replicates. Behavioral assays were replicated two or three times per time-point, depending on the experiment.

Statistical analysis

Results are expressed as mean values ± SEM and n values represent the number of animals in the experiment. Statistical analysis was carried out using Graphpad Prism 7 (GraphPad, prism software). The Kolmogorov– Smirnov and Levene's tests were used to test for normality and the equality of variances. A two-tailed unpaired Student's t-test, one-way ANOVA for evaluation of experiments with more than two groups, and one- or two-way repeated-measures ANOVA for functional assessments, were used. Tukey's, Sidak's or Fisher's LSD post-hoc tests were applied when appropriate. Behavioral assays were replicated two or three times, depending on the experiment, and averaged per animal. Statistics were then performed over the mean of animals. A threshold level of significance α was set at P<0.05. Significance levels were defined as follows: *p < 0.05; **p < 0.01; ***p < 0.001.

Supplementary Material

Refer to Web version on PubMed Central for supplementary material.

Acknowledgments:

References

1. Sofroniew MV, Dissecting spinal cord regeneration. Nature 557, 343–350 (2018). [PubMed: 29769671]

2. He Z, Jin Y, Intrinsic Control of Axon Regeneration. Neuron 90, 437–451 (2016). [PubMed: 27151637]

3. Di Giovanni S, Molecular targets for axon regeneration: focus on the intrinsic pathways. Expert Opin Ther Targets 13, 1387–1398 (2009). [PubMed: 19922299]

4. Xie F, Zheng B, White matter inhibitors in CNS axon regeneration failure. Exp Neurol 209, 302–312 (2008). [PubMed: 17706966]

5. Plunet W, Kwon BK, Tetzlaff W, Promoting axonal regeneration in the central nervous system by enhancing the cell body response to axotomy. J Neurosci Res 68, 1–6 (2002). [PubMed: 11933043]

6. Snider WD, Zhou FQ, Zhong J, Markus A, Signaling the pathway to regeneration. Neuron 35, 13–16 (2002). [PubMed: 12123603]

7. McQuarrie IG, Grafstein B, Gershon MD, Axonal regeneration in the rat sciatic nerve: effect of a conditioning lesion and of dbcAMP. Brain Res 132, 443–453 (1977). [PubMed: 199316]

8. Richardson PM, Issa VM, Peripheral injury enhances central regeneration of primary sensory neurones. Nature 309, 791–793 (1984). [PubMed: 6204205]

9. Neumann S, Woolf CJ, Regeneration of dorsal column fibers into and beyond the lesion site following adult spinal cord injury. Neuron 23, 83–91 (1999). [PubMed: 10402195]

10. Windhorst U, Muscle proprioceptive feedback and spinal networks. Brain Res Bull 73, 155–202 (2007). [PubMed: 17562384]

11. Akay T, Tourtellotte WG, Arber S, Jessell TM, Degradation of mouse locomotor pattern in the absence of proprioceptive sensory feedback. Proc Natl Acad Sci U S A 111, 16877–16882 (2014). [PubMed: 25389309]

12. Takeoka A, Vollenweider I, Courtine G, Arber S, Muscle spindle feedback directs locomotor recovery and circuit reorganization after spinal cord injury. Cell 159, 1626–1639 (2014). [PubMed: 25525880]

13. Lam T, Pearson KG, The role of proprioceptive feedback in the regulation and adaptation of locomotor activity. Adv Exp Med Biol 508, 343–355 (2002). [PubMed: 12171130]

14. Asboth L et al., Cortico-reticulo-spinal circuit reorganization enables functional recovery after severe spinal cord contusion. Nat Neurosci 21, 576–588 (2018). [PubMed: 29556028]

15. Formento E et al., Electrical spinal cord stimulation must preserve proprioception to enable locomotion in humans with spinal cord injury. Nat Neurosci, (2018).

16. van den Brand R et al., Restoring voluntary control of locomotion after paralyzing spinal cord injury. Science 336, 1182–1185 (2012). [PubMed: 22654062]

17. Wagner FB et al., Targeted neurotechnology restores walking in humans with spinal cord injury. Nature 563, 65–71 (2018). [PubMed: 30382197]

18. Alwis DS, Rajan R, Environmental enrichment and the sensory brain: the role of enrichment in remediating brain injury. Front Syst Neurosci 8, 156 (2014). [PubMed: 25228861]

19. Lopez-Atalaya JP et al., CBP is required for environmental enrichment-induced neurogenesis and cognitive enhancement. EMBO J 30, 4287–4298 (2011). [PubMed: 21847097]

20. Nithiananantharajah J, Hannan AJ, Enriched environments, experience-dependent plasticity and disorders of the nervous system. Nat Rev Neurosci 7, 697–709 (2006). [PubMed: 16924259]

21. Molteni R, Zheng JQ, Ying Z, Gomez-Pinilla F, Twiss JL, Voluntary exercise increases axonal regeneration from sensory neurons. Proc Natl Acad Sci U S A 101, 8473–8478 (2004). [PubMed: 15159540]

22. Wahl AS et al., Neuronal repair. Asynchronous therapy restores motor control by rewiring of the rat corticospinal tract after stroke. Science 344, 1250–1255 (2014). [PubMed: 24926013]

23. Tourtellotte WG, Milbrandt J, Sensory ataxia and muscle spindle agenesis in mice lacking the transcription factor Egr3. Nat Genet 20, 87–91 (1998). [PubMed: 9731539]

24. Ickes BR et al., Long-term environmental enrichment leads to regional increases in neurotrophin levels in rat brain. Exp Neurol 164, 45–52 (2000). [PubMed: 10877914]

25. Rattazzi L et al., Impact of Enriched Environment on Murine T Cell Differentiation and Gene Expression Profile. Front Immunol 7, 381 (2016). [PubMed: 27746779]

26. Bombeiro AL et al., Enhanced Immune Response in Immunodeficient Mice Improves Peripheral Nerve Regeneration Following Axotomy. Front Cell Neurosci 10, 151 (2016). [PubMed: 27378849]

27. Roth BL, DREADDs for Neuroscientists. Neuron 89, 683–694 (2016). [PubMed: 26889809]

28. Jin Q et al., Distinct roles of GCN5/PCAF-mediated H3K9ac and CBP/p300-mediated H3K18/27ac in nuclear receptor transactivation. EMBO J 30, 249–262 (2011). [PubMed: 21131905]

29. Henry RA, Kuo YM, Andrews AJ, Differences in specificity and selectivity between CBP and p300 acetylation of histone H3 and H3/H4. Biochemistry 52, 5746–5759 (2013). [PubMed: 23862699]

30. Hu SC, Chrivia J, Ghosh A, Regulation of CBP-mediated transcription by neuronal calcium signaling. Neuron 22, 799–808 (1999). [PubMed: 10230799]

31. Chrivia JC et al., Phosphorylated CREB binds specifically to the nuclear protein CBP. Nature 365, 855–859 (1993). [PubMed: 8413673]

32. Alarcon JM et al., Chromatin acetylation, memory, and LTP are impaired in CBP+/− mice: a model for the cognitive deficit in Rubinstein-Taybi syndrome and its amelioration. Neuron 42, 947–959 (2004). [PubMed: 15207239]

33. Thompson PR et al., Regulation of the p300 HAT domain via a novel activation loop. Nat Struct Mol Biol 11, 308–315 (2004). [PubMed: 15004546]

34. Yuan LW, Giordano A, Acetyltransferase machinery conserved in p300/CBP-family proteins. Oncogene 21, 2253–2260 (2002). [PubMed: 11948408]

35. Bangaru ML et al., Differential expression of CaMKII isoforms and overall kinase activity in rat dorsal root ganglia after injury. Neuroscience 300, 116–127 (2015). [PubMed: 25982557]

36. Chatterjee S et al., A novel activator of CBP/p300 acetyltransferases promotes neurogenesis and extends memory duration in adult mice. J Neurosci 33, 10698–10712 (2013). [PubMed: 23804093]

37. Chatterjee S et al., Reinstating plasticity and memory in a tauopathy mouse model with an acetyltransferase activator. EMBO Mol Med 10, (2018).

38. Lim JH et al., Neural activity promotes long-distance, target-specific regeneration of adult retinal axons. Nat Neurosci 19, 1073–1084 (2016). [PubMed: 27399843]

39. Jaiswal PB, English AW, Chemogenetic enhancement of functional recovery after a sciatic nerve injury. Eur J Neurosci 45, 1252–1257 (2017). [PubMed: 28244163]

40. Tedeschi A, Nguyen T, Puttagunta R, Gaub P, Di Giovanni S, A p53-CBP/p300 transcription module is required for GAP-43 expression, axon outgrowth, and regeneration. Cell Death Differ 16, 543–554 (2009). [PubMed: 19057620]

41. Gaub P et al., HDAC inhibition promotes neuronal outgrowth and counteracts growth cone collapse through CBP/p300 and P/CAF-dependent p53 acetylation. Cell Death Differ 17, 1392–1408 (2010). [PubMed: 20094059]

42. Gaub P et al., The histone acetyltransferase p300 promotes intrinsic axonal regeneration. Brain 134, 2134–2148 (2011). [PubMed: 21705428]

43. Puttagunta R et al., PCAF-dependent epigenetic changes promote axonal regeneration in the central nervous system. Nat Commun 5, 3527 (2014). [PubMed: 24686445]

44. Cho Y, Cavalli V, HDAC5 is a novel injury-regulated tubulin deacetylase controlling axon regeneration. EMBO J 31, 3063–3078 (2012). [PubMed: 22692128]

45. Cho Y, Sloutsky R, Naegle KM, Cavalli V, Injury-induced HDAC5 nuclear export is essential for axon regeneration. Cell 155, 894–908 (2013). [PubMed: 24209626]

46. Rossignol S, Frigon A, Recovery of locomotion after spinal cord injury: some facts and mechanisms. Annu Rev Neurosci 34, 413–440 (2011). [PubMed: 21469957]

47. Sandrow-Feinberg HR, Houle JD, Exercise after spinal cord injury as an agent for neuroprotection, regeneration and rehabilitation. Brain Res 1619, 12–21 (2015). [PubMed: 25866284]

48. Starkey ML et al., High-Impact, Self-Motivated Training Within an Enriched Environment With Single Animal Tracking Dose-Dependently Promotes Motor Skill Acquisition and Functional Recovery. Neurorehabil Neural Repair 28, 594–605 (2014). [PubMed: 24519022]

49. Jiang YQ, Zaaimi B, Martin JH, Competition with Primary Sensory Afferents Drives Remodeling of Corticospinal Axons in Mature Spinal Motor Circuits. J Neurosci 36, 193–203 (2016). [PubMed: 26740661]

50. Moraud EM et al., Mechanisms Underlying the Neuromodulation of Spinal Circuits for Correcting Gait and Balance Deficits after Spinal Cord Injury. Neuron 89, 814–828 (2016). [PubMed: 26853304]

51. Keeler BE et al., Acute and prolonged hindlimb exercise elicits different gene expression in motoneurons than sensory neurons after spinal cord injury. Brain Res 1438, 8–21 (2012). [PubMed: 22244304]

52. Gomez-Pinilla F, Ying Z, Zhuang Y, Brain and spinal cord interaction: protective effects of exercise prior to spinal cord injury. PLoS One 7, e32298 (2012). [PubMed: 22384207]

53. Molinari S et al., Deficits in memory and hippocampal long-term potentiation in mice with reduced calbindin D28K expression. Proc Natl Acad Sci U S A 93, 8028–8033 (1996). [PubMed: 8755597]

54. Sachdeva R, Theisen CC, Ninan V, Twiss JL, Houle JD, Exercise dependent increase in axon regeneration into peripheral nerve grafts by propriospinal but not sensory neurons after spinal cord injury is associated with modulation of regeneration-associated genes. Exp Neurol 276, 72–82 (2016). [PubMed: 26366525]

55. Kocsis JD, Waxman SG, Absence of potassium conductance in central myelinated axons. Nature 287, 348–349 (1980). [PubMed: 7421994]

56. Tanaka H, Ono K, Shibasaki H, Isa T, Ikenaka K, Conduction properties of identified neural pathways in the central nervous system of mice in vivo. Neurosci Res 49, 113–122 (2004). [PubMed: 15099709]

57. Kathe C, Hutson TH, McMahon SB, Moon LD, Intramuscular Neurotrophin-3 normalizes low threshold spinal reflexes, reduces spasms and improves mobility after bilateral corticospinal tract injury in rats. Elife 5, (2016).

58. Rishal I, Rozenbaum M, Fainzilber M, Axoplasm isolation from rat sciatic nerve. J Vis Exp, (2010).

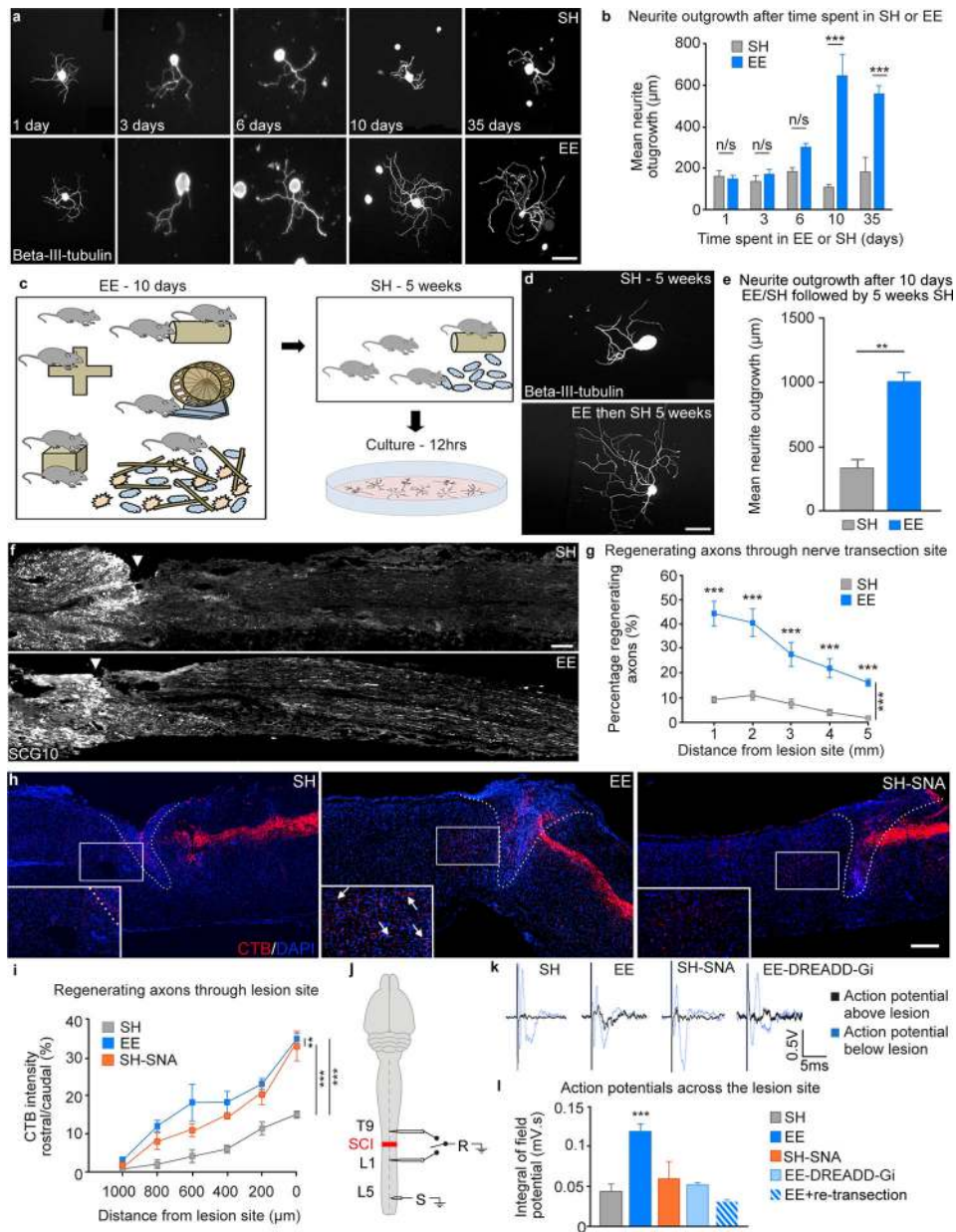**Fig. 1. Environmental enrichment induces a lasting increase in the regenerative potential of sensory neurons.**

A, Cultured mouse sciatic DRGs after exposure to EE, stained for Beta-III-tubulin. Scale bar 100 μm. **B,** Quantification of neurite outgrowth (mean ± SEM, Unpaired Student's t-tests ***P<0.001, n = 4/group). **C,** Diagram illustrating the experimental design, sciatic DRGs were cultured from mice that had been placed in EE for 10 days and then returned to SH for up to 5 weeks. **D,** Example images of sciatic DRGs from mice that had been in SH or EE for 10 days and then SH for 5 weeks. Scale bar 100 μm. **E,** Quantification of neurite outgrowth in DRGs from mice that had been exposed to EE compared to SH controls (mean ± SEM, unpaired Student's t test *** P<0.001, n = 4/group).**F,** Sciatic nerves immunostained for SCG10 after transection and re-anastomosis, Scale bar 500 μm. **G,** Quantification of

regenerating axons (mean ± SEM, Two-way ANOVA, Holm-Sidak post-hoc, ***P<0.001, **P<0.01, *P<0.05 n = 6/group). **H,** CTB-traced (red) dorsal column axons after injury, DAPI (blue), lesion site (dashed line). Scale bar, 200 μm. **I,** Quantification of CTB positive regenerating axons (mean ± SEM, Two-way repeated measures ANOVA, Tukey's post-hoc **P<0.01, ***P<0.001, n = 5/group). **J,** Electrophysiological setup. **K,** Representative compound action potentials recorded below (blue) and above (black) injury. **L,** Quantification of compound action potentials above the lesion (mean ± SEM, One-way ANOVA, Fisher's LSD post-hoc ***P<0.001, n = 4–7/group).
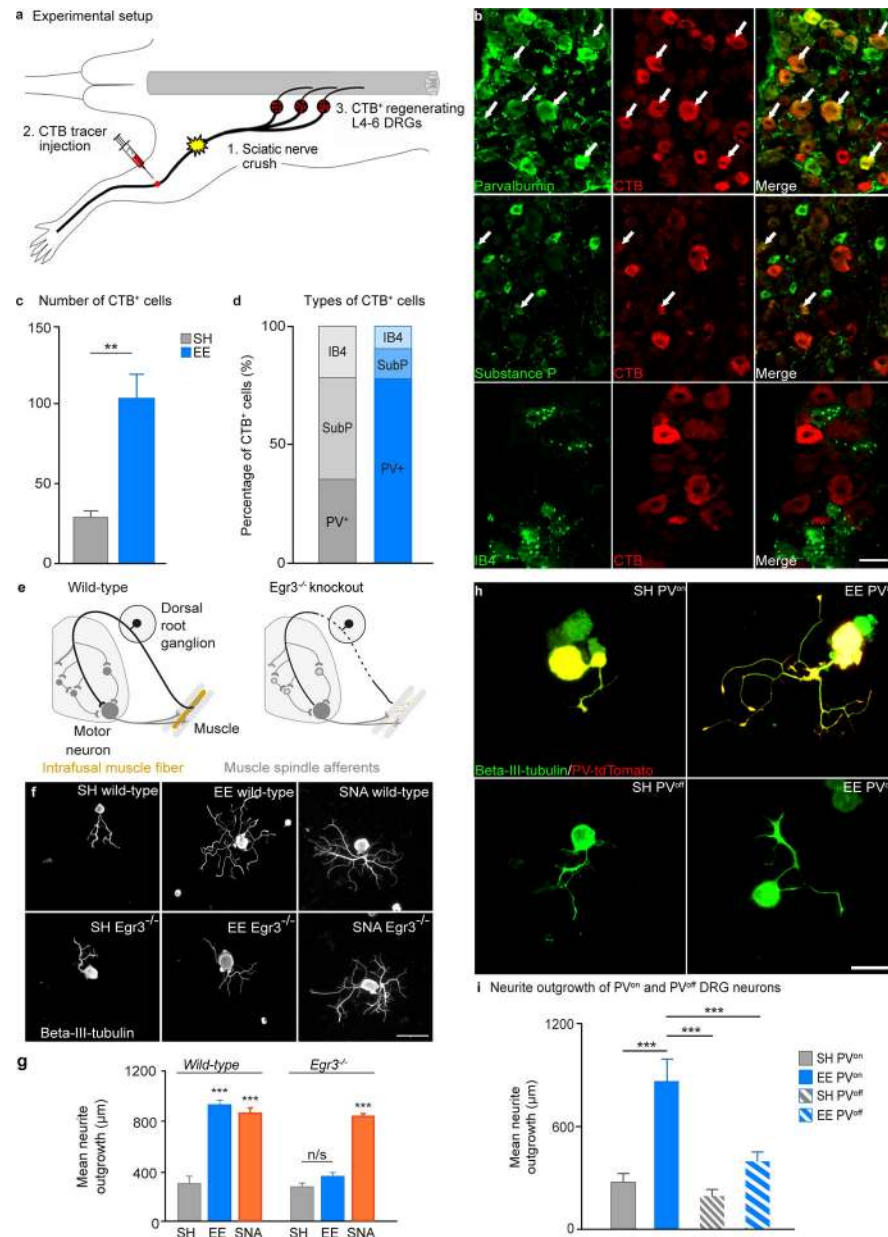
Fig. 2. Proprioceptive afferent feedback is required for EE-mediated increase in DRG regenerative growth.

A, Schematic of the experimental design, after EE and SH exposure mice underwent sciatic nerve crush injury and CTB injection distal to the crush site, axons that regenerate across the injury site take up CTB and retrogradely transport it to the soma. **B,** Representative images of co-localization between parvalbumin, substance P or isolectin B4 (green) and CTB (red) in DRGs from EE mice that had undergone a sciatic nerve crush. Scale bar, 50 μm. **C,** Quantification of the number of CTB positive DRG neurons in mice exposed to EE compared to SH (mean ± SEM, unpaired Student's t test, ** P<0.01, n = 6/group). **D,** Quantification of the percentage of CTB positive neurons that co-localized with parvalbumin, substance P or isolectin B4 after exposure to EE or SH. **E,** Schematic showing Egr3 mutation resulting in degeneration of muscle spindles. **F,** Beta-III-tubulin stained

sciatic DRGs from WT or *Egr3*⁻/⁻ mice after exposure to SH or EE. Scale bar 100 μm. **G,** Quantification of neurite outgrowth. (mean ± SEM, One-way ANOVA, Tukey's post-hoc, ***P<0.001, n = 4/group). **H,** Example images of tdTomato (red) positive or tdTomato negative DRGs co-stained with beta-III-tubulin (green) cultured from PV-cre x tdTomato mice that had been exposed to either SH or EE for 10 days. Yellow indicates colocalization between tdTomato and beta-III-tubulin. Scale bar 100 μm. **I,** Quantification of neurite outgrowth (mean ± SEM, One-way ANOVA, Tukey's post-hoc, ** P<0.01, *** P<0.001, n = 5/group).
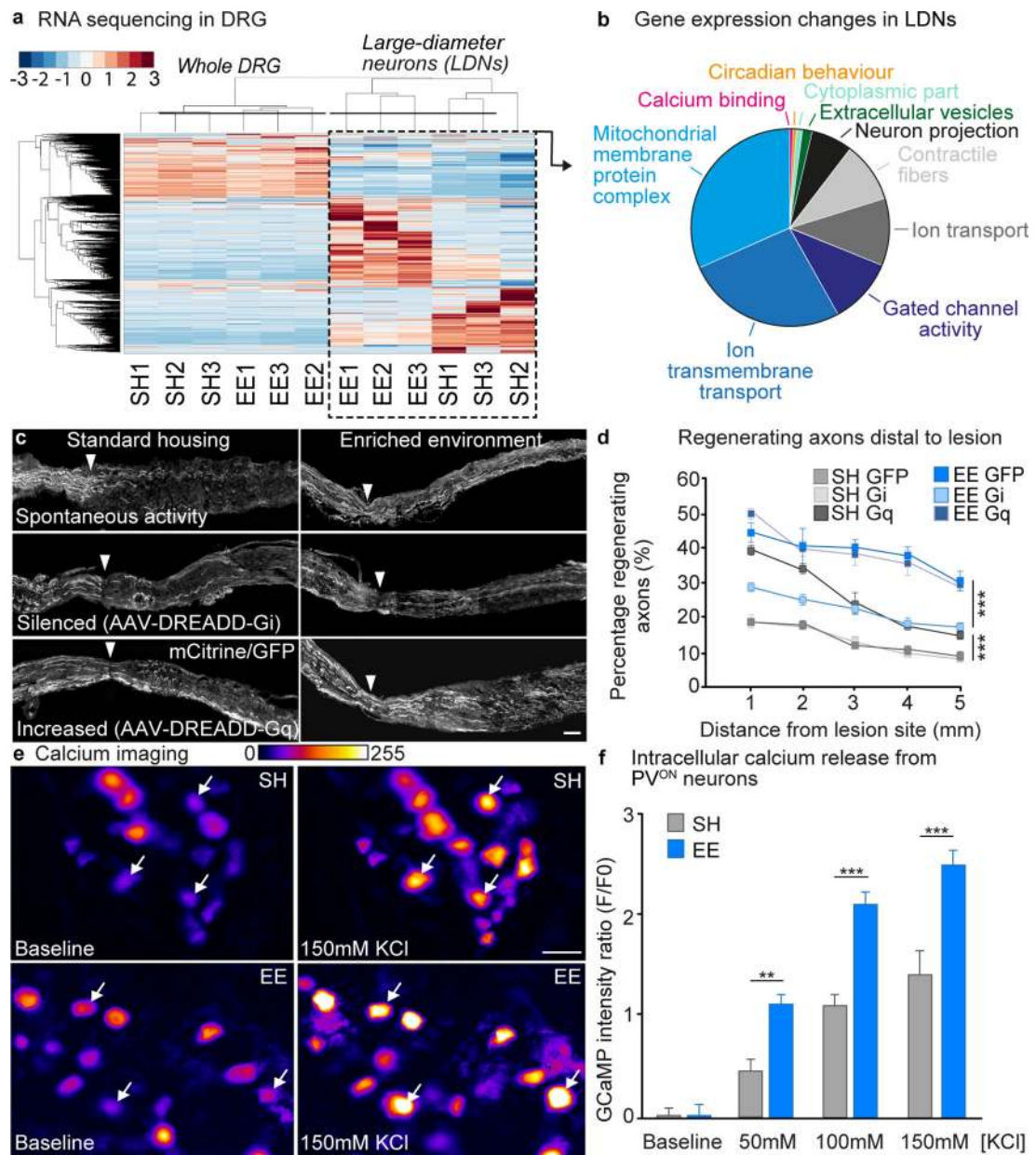
Fig. 3. EE induces signaling pathways involved in neuronal activity, calcium mobilization and the regenerative program of large-diameter DRG neurons.
A, Heatmap of the differentially expressed (DE) genes in whole-DRG and LDN RNA-seq (P<0.05). Color scale represents arbitrary expression units (lowest, blue; highest, red). **B,** Pie chart of genes in each functional group identified by GO analysis of DE genes in LDN. Functional groups are color-coded. **C,** Representative images of sciatic nerves transduced with AAV5-GFP, AAV5-hM4Di-mCitrine or AAV5-hM3Dq-mCitrine labeled with mCitrine/GFP after sciatic nerve crush. Arrow-head: lesion site. Scale bar, 500 μm. **D,** Quantification of axon regeneration (mean ± SEM, Two-way repeated measures ANOVA, Tukey's posthoc, ***P<0.001, n = 3/group). **E,** Representative time-lapse images of intracellular calcium release from whole-mount PV-GCaMP DRGs before and after addition of 150 mM KCl. Scale bar, 50 μm. **F,** Quantification of F/Fo ratio after 50 mM, 100 mM and

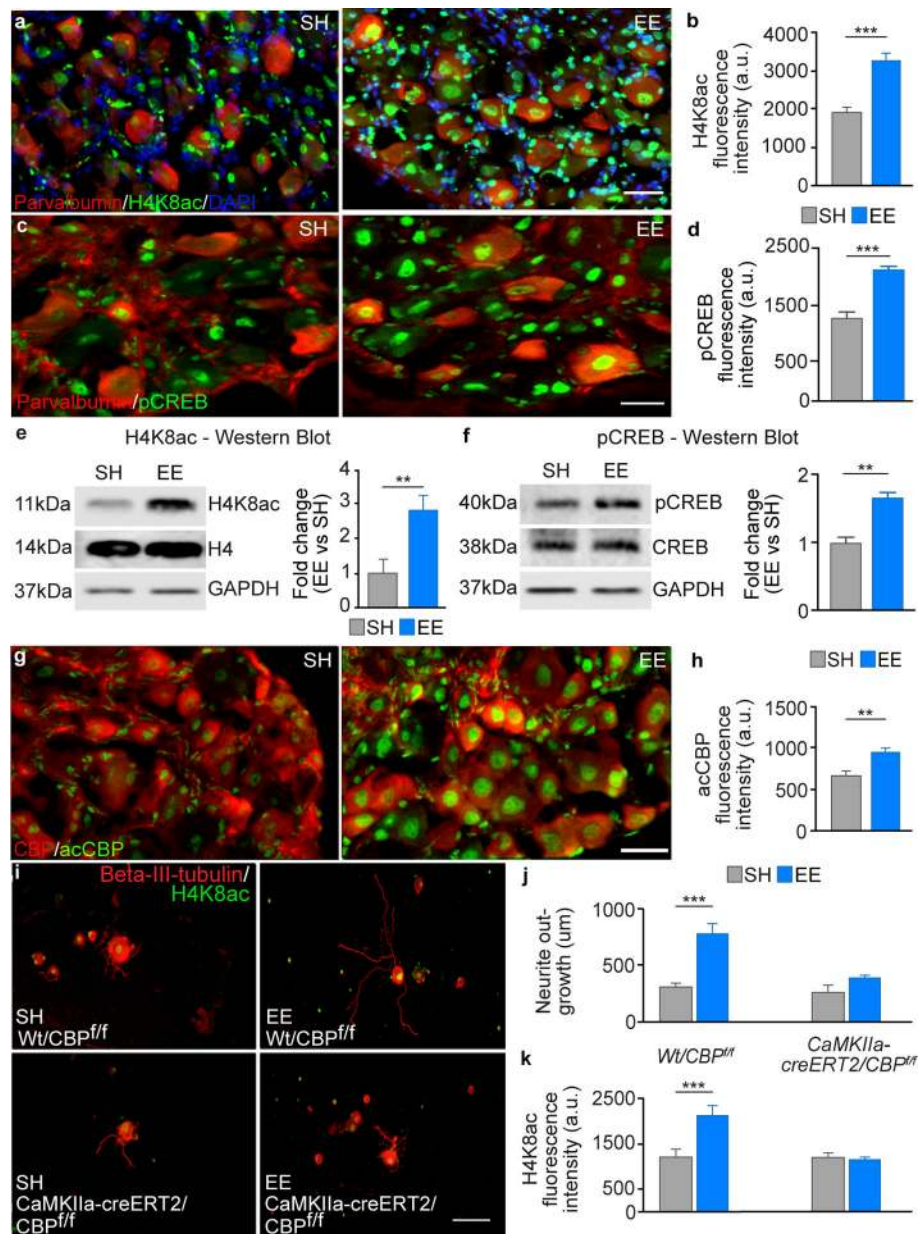150 mM KCl (mean ± SEM, Two-way ANOVA, Sidak's post-hoc **P<0.01, ***P<0.001, n = 4/group).

Fig. 4. Cbp is required for EE-dependent increase in regeneration potential.
A, DRGs stained for H4K8ac (green), parvalbumin (red) and DAPI (blue). Scale bar, 50 μm.
B, Quantification of H4K8ac intensity (mean ± SEM, unpaired Student's t test *** P<0.001, n = 6/group). **C,** Examples images of DRGs from mice housed in SH or EE, which were double stained for pCreb (green) and parvalbumin (red). Scale bar, 50 μm. **D,** Quantification of the fluorescence intensity of pCreb in the nuclei of parvalbumin positive DRGs (mean ± SEM, unpaired Student's t test *** P<0.001, n = 4/group). **E,** Immunoblotting analysis for H4K8ac from protein extracts from whole sciatic DRGs after 10 days exposure to SH or EE (mean ± SEM, unpaired Student's t test, ** P<0.01, n = 3/group). H4K8ac was normalised the levels of H4, Gapdh was used as a loading control. **F,** Immunoblotting analysis for pCreb from protein extracts of whole sciatic DRGs after 10 days exposure to SH or EE (mean ±

SEM, unpaired Student's t test ** P<0.01, n = 3/group). pCreb was normalised to levels of Creb; Gapdh was used as a loading control. **G,** DRGs stained for acCbp (green) and total Cbp (red). Scale bar, 50 μm. **H,** Quantification of acCbp intensity (mean ± SEM, unpaired Student's t test *** P<0.001, n = 11/group). **I,** Cultured DRG neurons from WT x Cbp$^{f/f}$ or CaMKIIa-creERT2 x Cbp$^{f/f}$ mice (Beta-III-tubulin, red and H4K8ac, green). Scale bar, 200 μm. **J,** Quantification of neurite outgrowth (mean ± SEM, One-way ANOVA, Tukey's post-hoc *** P<0.001, n = 5/group). **K,** Quantification of H4K8ac intensity (mean ± SEM, One-way ANOVA, Tukey's post-hoc *** P<0.001, n = 5/group).
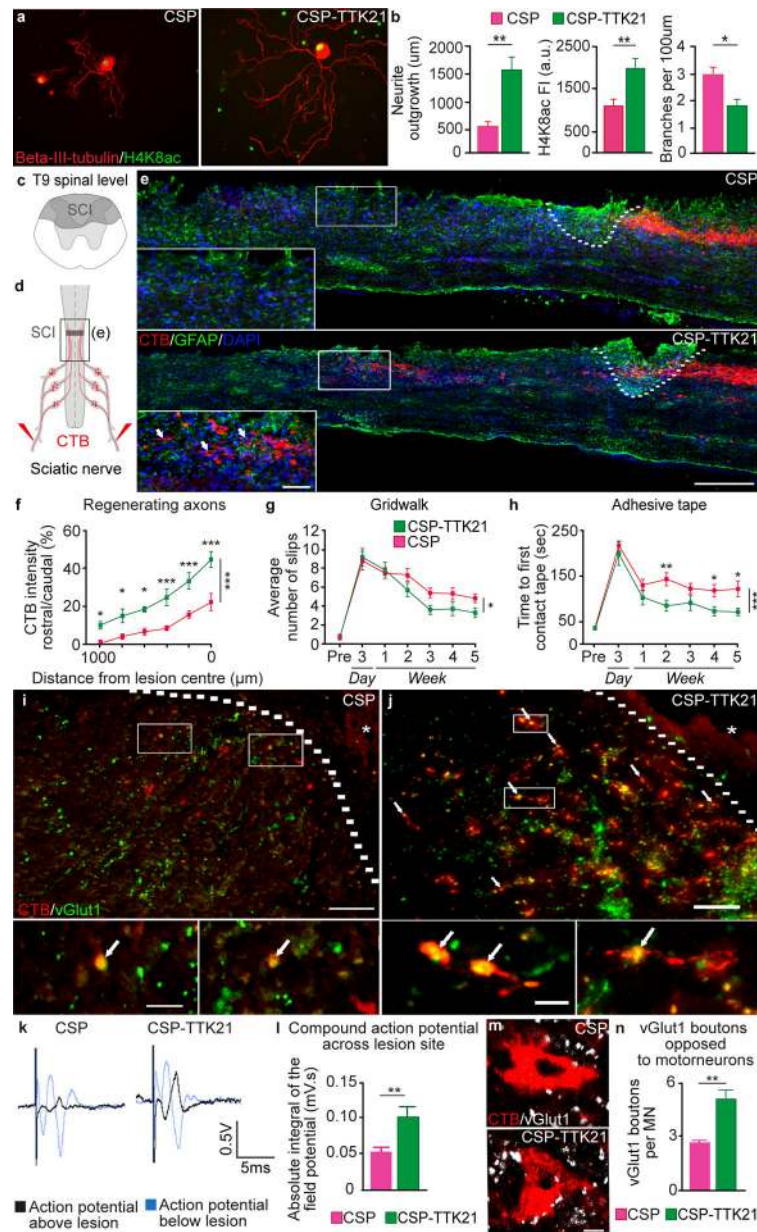
Fig. 5. Pharmacological activation of Cbp/p300 promotes sensory axon regeneration and recovery after a dorsal hemisection SCI in mice.

A, Cultured DRG neurons treated with control (CSP) or Cbp/p300 pharmacological activator (CSP-TTK21) (Beta-III-tubulin, red and H4K8ac, green). Scale bar, 50 μm. **B,** Quantification of neurite outgrowth (mean ± SEM, unpaired Student's t test **P<0.01, n = 4/group), H4K8ac intensity (mean ± SEM, unpaired Student's t test **P<0.01, n = 11/group) and neurite branching (mean ± SEM, unpaired Student's t test *P<0.05, n = 4/group) **C,** Schematic view of a T9 dorsal column axotomy that lesions the ascending sensory axons in the dorsal columns. **D,** CTB (red) was injected into the sciatic nerve 5 weeks after SCI. **E,** CTB-traced (red) dorsal column axons after SCI, Gfap (green), DAPI (blue), lesion site (dashed line). Scale bar, 200 μm. **F,** Quantification of CTB positive regenerating axons (mean ± SEM, Two-way repeated measures ANOVA, Holm's Sidak post-hoc ***P<0.001,

P<0.01, *P<0.05, n = 5/group). **G, Quantification of slips (mean ± SEM, Two-way repeated measures ANOVA, Fisher's LSD post-hoc *P<0.05, n = 10/group). **H,** Quantification of the time required to first contact an adhesive pad placed on the hindpaws (mean ± SEM, Two-way repeated measures ANOVA, Fisher's LSD post-hoc ***P<0.001, **P<0.01, *P<0.05, n = 10/group). **I,** Representative image from a control CSP treated mouse showing CTB-positive regenerating axons rostral to the lesion and co-localization with the pre-synaptic marker vGlut1. Lesion site is marked by the dashed line and asterisk. Scale bar, 100 μm, scale bar for insets 10 μm. **J,** Representative image from a CSP-TTK21 treated mouse showing co-localization of regenerating CTB (red) positive axons rostral to the spinal cord injury site (marked by the dashed line and asterisk) with the pre-synaptic marker vGlut1 (green) to identify prospective nascent synapses (marked by arrows). Scale bar, 100 μm. Higher-magnification images of insets show co-localization of CTB positive axons (red) and vGlut1 (green). Scale bar, 10 μm. **K,** Quantification of CTB and vGlut1 co-localization rostral to the lesion site (mean ± SEM, unpaired Student's t test ***P<0.001, n = 6/group). **L,** Representative compound action potentials recorded below (grey) and above (black) the lesion. **M,** Quantification of compound action potentials above the lesion (mean ± SEM, unpaired Student's t test *P<0.05, n = 8–10/group). **N,** vGluT1 positive boutons (white) from Group-Ia afferents in proximity to hindlimb motoneurons (Red, CTB) below the injury (L1–4). Scale bar, 25 μm. **O,** Quantification of vGluT1 positive boutons opposed to motoneurons (mean ± SEM, unpaired Student's t test **P<0.01, n = 8/group).
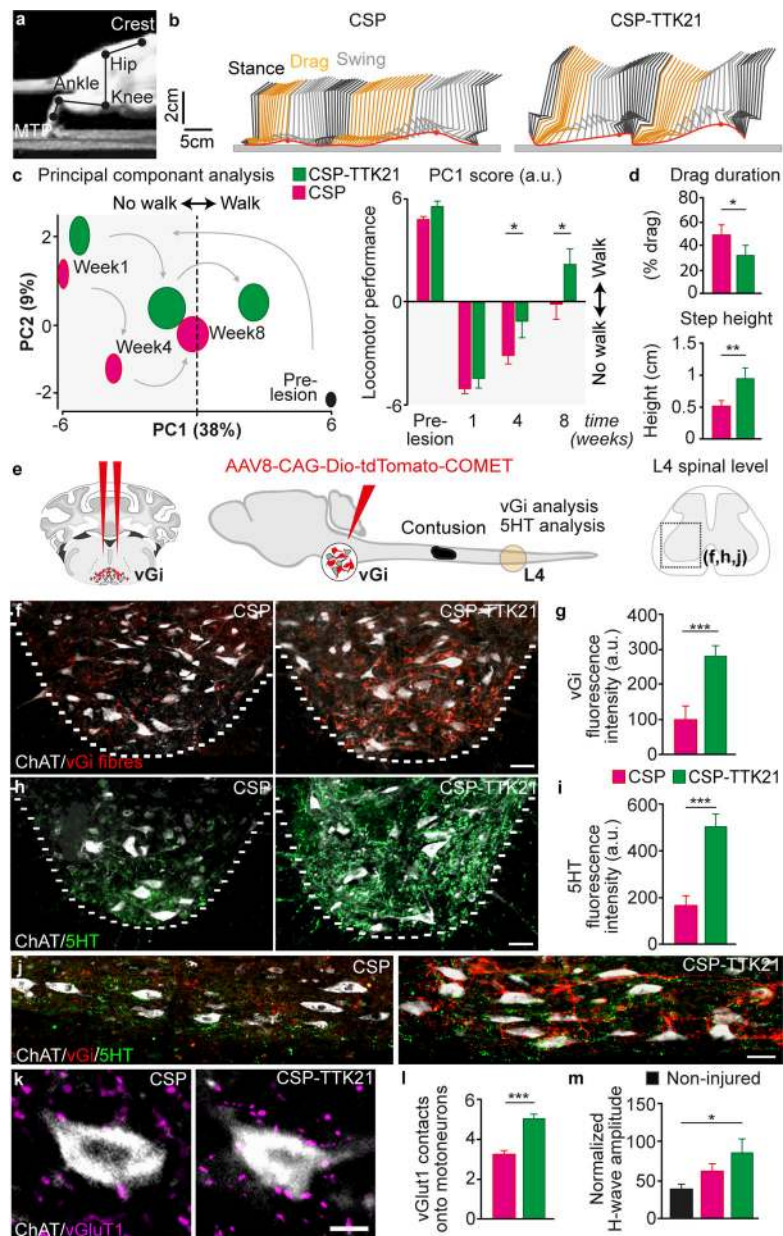
Fig. 6. Pharmacological Cbp/p300 activation enhances sprouting of both descending motor and ascending sensory axons leading to functional recovery after contusion SCI in rats.

A, Image showing joints used for reconstruction of hindlimb movements **B,** Representative hindlimb kinematics after treatment with CSP or CSP-TTK21. Black, orange and grey correspond to stance, drag and swing phases of gait, respectively. **C,** PC analysis of gait parameters averaged for each group at weeks 1, 4 and 8 and quantification of average scores on PC1, which quantify the locomotor performance of rats treated with CSP or CSP-TTK21 (mean ± SEM, Two-way ANOVA, Fisher's LSD post-hoc * P<0.05, n = 10/group). **D,** Bar plots of drag duration and step height (mean ± SEM, unpaired Student's t test * P<0.05, **P<0.01, n = 10/group). **E,** Schematics showing strategy for tracing vGi axons, T9 contusion and the L4 ventral horn analyzed for vGi and 5HT sprouting. **F,** Representative images of descending vGi axons (Red) sprouting around motoneurons (ChAT, Cyan) in the

lumbar ventral horn after treatment with CSP or CSP-TTK21. Scale bar, 50 μm. **G,** Quantification of vGi intensity in the ventral horn (mean ± SEM, unpaired Student's t test, ***P<0.001, n = 8/group). **H,** Representative images of descending 5HT axons (Magenta) sprouting around motoneurons (ChAT, Cyan) in the lumbar ventral horn after treatment with CSP or CSP-TTK21. Scale bar, 50 μm. **I,** Quantification of 5HT intensity in the ventral horn (mean ± SEM, unpaired Student's t test, ***P<0.001, n = 9/group). **J,** Representative sagittal sections showing sprouting of descending vGi (Red) and 5HT (Green) axons around motoneurons (ChAT, White) below in the injury in the lumbar ventral horn after treatment with CSP or CSP-TTK21. Scale bar, 50 μm. **K,** vGluT1 positive boutons (yellow) from Group-Ia afferents in proximity to motoneurons (ChAT, Cyan) below the injury (L1–4). Scale bar, 25 μm. **L,** Quantification of vGluT1 positive boutons opposed to motoneurons (mean ± SEM, unpaired Student's t test ***P<0.001, n = 9/group). **M,** Quantification of the H-wave amplitude after treatment with CSP or CSP-TTK21 (mean ± SEM, One-way ANOVA, Tukey's post-hoc * P<0.05, n = 5–10/group).